



OPEN

Genet identity and season drive gene expression in outplanted *Acropora palmata* at different reef sites

Benjamin D. Young^{1,2,3✉}, Dana E. Williams^{1,4}, Allan J. Bright^{1,4}, Annie Peterson^{1,4}, Nikki Taylor-Knowles³ & Stephane M. Rosales^{1,2}

Coral reefs are experiencing decreases in coral cover due to anthropogenic influences. Coral restoration is addressing this decline by outplanting large volumes of corals onto reef systems. Understanding how outplanted corals react at a transcriptomic level to different outplant locations over time is important, as it will highlight how habitat affects the coral host and influences physiological measures. In this study, the transcriptomic dynamics of four genets of outplanted *Acropora palmata* were assessed over a year at three reef sites in the Florida Keys. Genet identity was more important than time of sampling or outplant site, with differing levels of baseline immune and protein production the key drivers. Once accounting for genet, enriched growth processes were identified in the winter, and increased survival and immune expression were found in the summer. The effect of the reef site was small, with hypothesized differences in autotrophic versus heterotrophic dependent on outplant depth. We hypothesize that genotype identity is an important consideration for reef restoration, as differing baseline gene expression could play a role in survivorship and growth. Additionally, outplanting during cooler winter months may be beneficial due to higher expression of growth processes, allowing establishment of outplants on the reef system.

Keywords *Acropora palmata*, RNA-seq, Coral restoration, Florida keys, Immune gene expression

Despite their biological and economic importance, tropical coral reefs are in decline because of local and global anthropogenic influences^{1–3}. At local scales, factors such as pollution and increased nutrient run-off are decreasing coral fitness making them more susceptible to disease and bleaching events^{4–7}. At a global scale, anthropogenic climate change is further causing deleterious problems through ocean warming^{3,8,9} and ocean acidification^{10–12}. Global and local stressors do not act alone, with the synergistic effects of these variables^{2,10,13,14} further reducing coral host fitness, and causing phase shifts from coral to algal reef systems^{15–17}.

One area trying to stem the decline of tropical coral reefs is coral restoration which restores stony corals to the reef ecosystem^{18–20}. Coral restoration has grown substantially since the early 2000s, with large biomasses of corals outplanted to reef systems^{18,21}. Historically, asexual propagation has been the primary focus of restoration activities and involves fragging larger colonies into smaller pieces which show increased growth rates compared to larger colonies^{22,23}. These fragged pieces of coral are then replanted on the reefs in clusters allowing fusion, resulting in large coral colonies being formed over a markedly shorter time frame^{22,24}. Recently, this method has shown success, with fused outplanted corals subsequently spawning^{25,26}. The increase in coral biomass for restoration activities has led to the need to research optimal outplant sites for restoration success. Outplant sites can vary in their morphology (a flat reef structure versus a spur and groove system) and the abiotic conditions they exhibit^{27–29}. With different coral species exhibiting habitat preferences^{30–32}, outplant site is a key consideration for restoration. Additionally, within species variability also needs to be considered. For example, different genets from a coral species can vary in bleaching resistance^{33,34}, disease resistance^{35,36}, and growth capabilities^{37–39}. The exact mechanisms driving differences between genet responses within a species are

¹Cooperative Institute of Marine and Atmospheric Science, Rosenstiel School of Marine, Atmospheric, and Earth Science, University of Miami, Miami, FL, USA. ²Atlantic Oceanographic and Meteorological Laboratory, National Oceanic and Atmospheric Administration, Miami, FL, USA. ³Department of Marine Biology and Ecology, Rosenstiel School of Marine, Atmospheric and Earth Science, University of Miami, Miami, FL, USA. ⁴Southeast Fisheries Science Center, National Oceanic and Atmospheric Administration-National Marine Fisheries Service, Miami, FL, USA. ✉email: benjamindouglasyoung1993@gmail.com

multifaceted and may involve the coral host genetics and its microbiome (prokaryotes, viruses, Symbiodiniaceae, protists, and fungi). For the coral host factors influencing gene expression, such as epigenetic modification^{40,41}, gene frontloading^{42,43}, and genetic mutations^{44,45} could be important in shaping differences between genets, leading to varying levels of baseline gene expression. We hypothesize that this may lead to specific processes, such as immune responses, being naturally higher in some genets providing increased resistance to factors such as pathogens. Therefore, baseline gene expression may play a key role in predicting resistance and susceptibility, as well as performance for outplanted corals at different reef habitats. By understanding the underlying stressors that coral may encounter at an outplant site, preferential genets can be selected to maximize survivability and growth in restoration activities.

In the Caribbean, one species heavily focused on for restoration activities is the critically endangered branching coral *Acropora palmata*^{46–48}. In the Florida Keys, since the 1980's, this species has seen drastic declines due to disease outbreaks^{49,50}, bleaching events^{51,52}, and human influences⁵³. Due to the fast-growing nature of *A. palmata*, it is especially conducive to asexual fragmentation⁵⁴ allowing large biomass to be accrued and outplanted onto the reefs. Despite the Coral Restoration Foundation (CRF) prioritizing *A. palmata* as a key coral species for outplanting, there has so far been no research on how different reef sites influence the transcriptomic profiles of different *A. palmata* genets. Understanding the transcriptomic profiles will allow the identification of potential resistant and susceptible genets and underlie the importance of fully characterizing reef site conditions to improve survivability of outplanted corals.

In this study, we characterized the gene expression profiles over a year of multiple fragments of four genets of *A. palmata* at three reef sites in the Florida Keys with ongoing active restoration: Carysfort Reef, Pickles Reef, and North Dry Rocks (Fig. 1A). We found that genet identity was the largest driver of the gene expression, swamping any signal of reef site or sampling time (i.e., time of year). We also found differences in gene expression of baseline immune activity and metabolic activity between the genets. Once accounting for genet identity, we identified significantly correlated co-expression modules linked to the different sampling times, with these modules linked to the cooler winter months, and hotter summer months.

Materials and methods

Field site selection

Three active restoration field sites in the Northern Florida Keys, managed by the Coral Restoration Foundation (CRF), were chosen for field sampling: Carysfort Reef (25.2209, −80.2102), Pickles Reef (24.9845, −80.4164), and

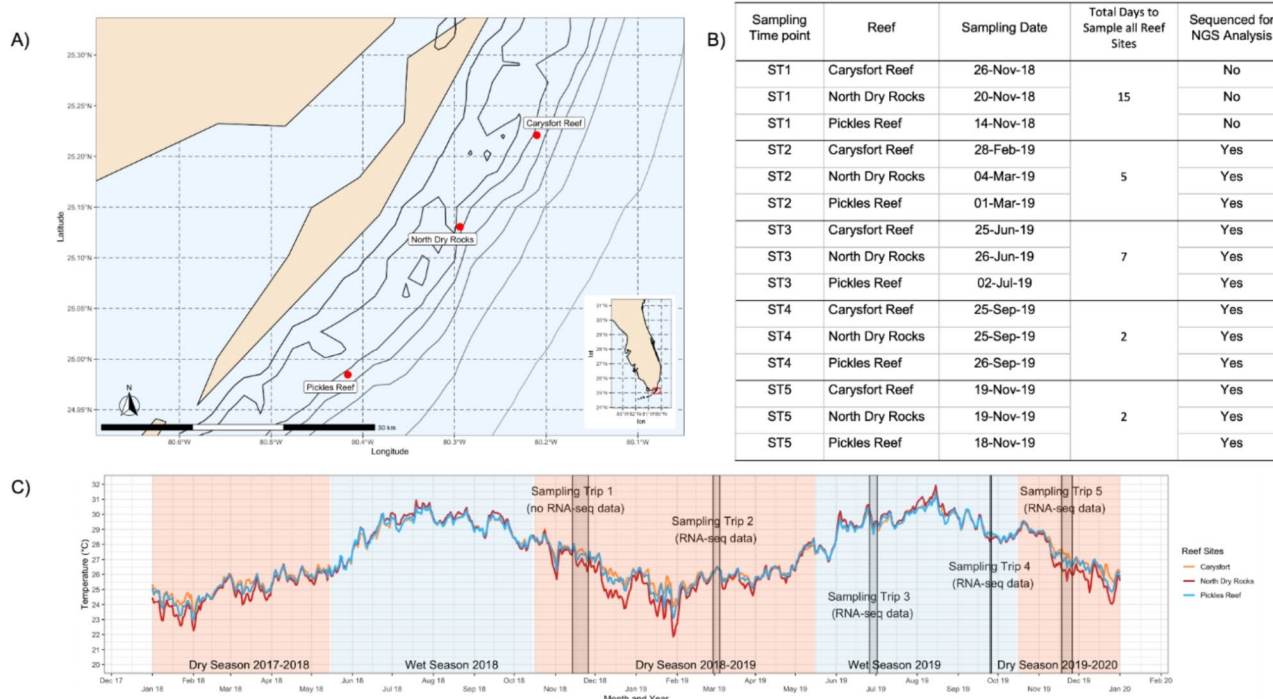


Fig. 1. Reef location, outplant sampling summaries, and sea surface temperatures (SST) for the three reef sites. (A) Locations of the three reef sites in the Florida Keys denoted by red dots. Inset map bottom right identifies the location with a square box of the main map image. (B) Field sampling summaries and samples selected for RNA-seq analysis. The table shows each sampling time point (ST; column 1), reef site (column 2), date of sampling (column 3), the total number of days to sample all reef sites for each sampling time point (column 4), and which subset of sampling time points were selected for RNA-seq analysis. (C) Plot of OISST at the three reef sites studied (colored lines). Seasons are indicated on the figure by blue fill (wet season) and red (dry season). Sampling time point ranges are indicated by black vertical bars on the plot.

North Dry Rocks (25.1304, -80.2940) (Fig. 1A). Carysfort Reef was the northernmost sampling site (Fig. 1A), a shallow reef system with low rugosity. Sampled *A. palmata* outplants were located between 17 and 22 ft. North Dry Rocks was the middle sampling site (Fig. 1A), a spur and groove reef system. All sampled *A. palmata* were located on one spur and ranged from 10 to 15 ft in depth. Pickles Reef was the most southern sampling site (Fig. 1A) with low rugosity like Carysfort Reef, with sampled corals between 14 and 19 ft. These three reef sites provided different latitudinal locations, and different outplant depths of *A. palmata* for correlative analysis.

Coral sampling

Five sampling time points were conducted at each of the three reef sites: sampling time point one (ST1) during November 2018, sampling time point two (ST2) during February/March 2019, sampling time point three (ST3) during June/July 2019, sampling time point four (ST4) during September 2019, and sampling time point five (ST5) during November 2019 (Fig. 1B). These covered a full year and the summer and winter months. For each sampling time point, all reefs were sampled in a 7-day period (Fig. 1B) with SCUBA used to access outplanted *A. palmata* fragments within clusters. Each cluster contained six to seven fragments of the same genet and clusters were identified for each sampling time point using cow tags placed at initial outplanting (Supplementary Fig. S1). For each sampling time point, clusters underwent health surveys and tissue sampling using a hammer and chisel. In each cluster, three of the six to seven fragments were sampled at each sampling time point, with the same fragments sampled between sampling timepoints using unique numeric identifiers and previously taken outplant cluster photographs. A tissue sample was then collected in pre-labeled zip bags with SCUBA, with tools wiped between samples. On the boat, tissue samples were transferred to 2 ml cryovial tubes filled with 1.5 ml of RNAlater and placed on ice. All tissue samples were processed and placed on ice within 35 min of sampling. All tools used in transferring tissue samples were bleached and wiped down with ethanol between each sample. At the end of each day, samples were placed at -80 °C.

Sea surface temperature for the reef sites

Sea surface temperature (SST) was obtained from the National Oceanographic and Atmospheric Association (NOAA) Optimum Interpolation Sea Surface Temperature (OISST) data set^{55–57}. To cover all sampling timepoints, data was subset for a temporal range from October 2018 to January 2020 and obtained for each reef site. OISST time course plotting was undertaken in R (v4.0.3) and RStudio (v1.4.1106) using tidyverse⁵⁸ and GGPplot2⁵⁹. Average temperatures were calculated across all reef sites, as well as average temperature recorded at each reef site for each sampling time point. The average temperature was also calculated for each reef site and the time span it took to sample all reefs at each sampling time point.

Sample choice for sequencing

A total of 1227 samples of 11 genets of *A. palmata* were collected from the three reef sites over the five sampling timepoints. Of the 11 genets sampled, four were selected for further processing. These genotypes were selected since they were used in an *ex-situ* disease experiment⁶⁰ and are referred to using CRF designations: CN2, CN4, ML2, and HS1. As high replication of genets within each reef was desired, only four of the five sampling timepoints were chosen for sequencing: ST2 (February/March 2019), ST3 (June 2019), ST4 (September 2019), and ST5 (November 2019). This resulted in 380 samples of *A. palmata* for 3' RNA-sequencing, with full reef, genet, and timepoint breakdown available in Supplemental File S1.

RNA extractions, complementary DNA synthesis, and sequencing

The 380 samples chosen for RNA-seq library prep were randomized to minimize bias due lab work and variables of interest (e.g. sampling time point, reef location). DNA and RNA were extracted from the same piece of coral tissue using the Zymo MagBead DNA/RNA kit on the Kingfisher Flex. For an in-depth protocol please see⁶¹. On completion, eluted DNA was placed at -80 °C for amplicon sequencing. For eluted RNA, 8 µl aliquots were used for quality control (nanodrop and qubit), with the remainder sealed and placed at -80 °C for downstream processing.

Total RNA was converted to complementary DNA (cDNA) using the Quant-seq FWD kit (Lexogen) following the high yield/quality manufacturers protocol. The qPCR add-on kit (Lexogen) was utilized to ascertain the RNA concentrations needed to reduce under and over PCR cycling. Samples were dual indexed and sent to the Hussman Institute for Human Genomics (Miller School of Medicine, University of Miami) for single-end (SE) 100 sequencing on a NOVA-seq utilizing two lanes. Sample read depth was requested at 4–5 million reads.

Transcriptomic bioinformatics

Pre-processing of the 3'RNA-seq libraries followed the same pipeline as⁶⁰. Demultiplexing was done by the sequencing facility, and raw reads had adapters and low-quality reads trimmed using BBduk.sh⁶² with recommended parameters from Lexogen (<https://www.lexogen.com/quantseq-data-analysis>). FastQC⁶³ was then used to identify successful removal of low-quality reads and adapters for all samples. Alignment and quantification utilized Salmon⁶⁴ and the annotated *A. palmata* transcriptome^{65,66}. Quantified samples were read into R (v4.0.3) and RStudio (v1.4.1106) using tximport⁶⁷ and quantified to the gene level. Samples with less than 1,000,000 total read counts, and genes with less than four counts in greater than 15 samples, were removed. This filtering criteria was used as it retained ~ 16,000 genes for downstream analyses, while also being conservative only removing extremely lowly expressed genes and allowing any differences due to rare genes within treatments to be maintained.

Prior to analysis, hierarchical clustering using hclust⁶⁸ was employed to identify any sample groupings that were not explained by available metadata and thus deemed as surrogate variables. Downstream analysis either removed the surrogate variable or incorporated it in statistical models.

Principal component analysis (PCA) was run using a variance stabilized transformation (VST) of the raw counts, on all coral samples, using a modified PlotPCA function from DeSeq2 (v 1.40.2)⁶⁹. Correlations of principal components (PCs) to metadata variables were done using pcatoools::eigencorplot⁷⁰, with significance identified using a Pearson correlation. Visualization of PCs of interest was done using GGPlot2⁵⁹. To identify finer scale patterns, surrogate/batch variables were removed using limma::removeBatchEffect⁷¹ on the VST of raw counts. The batch corrected VST data was then used as input for additional PC analysis.

Differential gene expression (DGE) analysis was run using DeSeq2 (v 1.40.2)⁶⁹. To identify differences in baseline gene expression between the four genets (ML2, CN2, CN4, and HS1) the Likelihood Ratio Test (LRT) methodology was used. The full model (\sim Surrogate Variable + Sampling Timepoint + Genet) and reduced (\sim Surrogate Variable + Sampling Timepoint), were used, with alpha set to 0.001. All significant genes were used in gene ontology (GO) and Kyoto Encyclopedia of Genes and Genomes (KEGG) pathway enrichment analysis. To identify finer scale expression profiles between the genets, the VST counts of significant genes from the LRT were used in DEGreport::degpatterns⁷². Visualization of identified gene clusters was done in GGplot2⁵⁹, and GO and KEGG enrichment analysis was undertaken for all identified clusters. Due to high enrichment of neurodegenerative disease terms, Venn diagram analysis was undertaken to identify the level of overlap of the genes present within these terms for relevant clusters.

Weighted gene co-expression network analysis (WGCNA) was run using the r package WGCNA⁷³. To identify co-expression due to sampling time point and reef, input for WGCNA analysis was the VST transformed counts with genet and surrogate variable variance removed using limma::removeBatchEffect. Outlier samples were identified using the Ward.D2 methodology, and a single signed network was constructed manually with the following key parameters: softPower = 8, minModuleSize = 30, deepSplit = 2, mergedCutHeight = 0.25, minimumVerbose = 3, and cutHeight = 0.997 (Supplementary Fig. 2). The eigengene values of each module were correlated to sampling timepoints (ST2, ST3, ST4, and ST5), OISST SST, reef sites (CF, NDR, and PI), and outplant depth. For the OISST SST, we used the respective daily average temperature value for each sampling time point at each reef site, with this data available in Supplementary File S2. The highest connected gene within each module was also identified (wgcna::chooseTopHubInEachModule). GO and KEGG enrichment analysis was done for each module to ascertain putative biological functions and roles. Interesting modules were then subset from the main wgcna heatmap, and manually arranged for visualization, using ComplexHeatmap⁷⁴.

Significant gene lists (from DEseq2), clusters (from DEGpatterns), and modules (from WGCNA) were used as input for GO enrichment analysis in Cytoscape v.3.8.2⁷⁵ and the application BiNGO⁷⁶. Enrichment analysis was run using the hypergeometric test and p-value correction using a Benjamini & Hochberg false discovery rate (FDR). Alpha was set at 0.01 for all GO enrichment analyses. The background universe of genes to test enrichment was the set of genes remaining after initial low count filtering. Visualization of GO enrichment was done in Cytoscape v3.8.2⁷⁵, and further visualization of gene expression to GO terms was run in the R package Complex Heatmap⁷⁴ using the VST counts with genet and batch variable removed.

Significant gene lists (from DEseq2), clusters (from DEGpatterns), and modules (from WGCNA) were also annotated with their KEGG gene identifiers present in the *A. palmata* annotation file^{65,66}. Clusterprofiler v3.18.1⁷⁷ was used to identify KEGG pathway enrichment, with enrichment tested against the KEGG Orthology database (organism = “ko”), and alpha set at 0.01. Visualization of enriched pathways was done with clusterprofiler⁷⁷, enrichPlot 1.10.2⁷⁸, GGPlot2⁵⁹ and complex heatmap⁷⁴.

For clusters (identified from DEGpatterns), and modules (identified from WGCNA), significant GO and KEGG enrichment results were inspected and used to assign putative overarching functions. We present full significant KEGG and GO results used to assign these putative functions in supplementary files.

Results

Sea surface temperature between the three reef sites

There were minimal differences in temperature profiles at each sampling time point for the three reef sites over the one-year period (Fig. 1C). Seasonally, November 2018 to May 2019 showed average temperatures of \sim 26 °C. May 2019 onwards showed an increase in temperature, with average values around 30 °C and a max in mid-August 2019 of 32 °C. September 2019 onwards saw a decrease back to \sim 26 °C. Due to weather conditions, reefs were sampled at each time point as close as feasibly possible. For ST1 this covered 15 days (14th–26th November 2018), ST2 five days (28th February to 4th March 2019), ST3 seven days (25th June–2nd July 2019), ST4 two days (25th–26th September 2019), and ST5 two days (18th–19th November 2019) (Fig. 1B). For each reef site and sampling time point, the average OISST SST is reported in Table 1.

Sequencing results

A total of 374 of the 380 samples were successfully sequenced (Supplemental File S1), with sample read depth ranging from 567,208 to 16,494,255 reads, and an average and median read depth of 1,843,913 (standard deviation (SD) = 1,281,721) and 1,550,645 respectively, and an average alignment to the *A. palmata* annotated transcriptome of 32.95% which was expected and similar to previous 3'RNA-seq alignment rates in the species⁶⁰. A total of 12 samples were removed with $<$ 1 million counts across all genes. This resulted in average and median read depths of 1,877,383 (SD = 1,288,203) and 1,563,692 respectively, and 362 samples for downstream analysis (Supplemental File S1). When grouping by genet, this resulted in the following sample size: CN2 = 108, CN4 = 77, HS1 = 102, and ML2 = 75. For a breakdown of sampling time point and reef site sample sizes, please see Table 1. Initial hierarchical clustering of the samples identified a strong surrogate variable which was not explained by any metadata variables taken (Supplementary Fig. S3). As such, all downstream differential expression and co-expression analysis included this as a surrogate effect. Filtering of low count genes resulted in 15,767 genes being retained for downstream analysis. These 15,767 genes also constituted the ‘gene universe’ (i.e. background set of genes used to test enrichment for gene lists of interests) used for GO enrichment analysis. While 3' RNA-

Reef site	Sampling time point	OISST average temperature sea surface temperature (°C)	Samples used in transcriptomic analysis
Carysfort reef	ST1	27.01	n/a
	ST2	26.20	27
	ST3	30.15	24
	ST4	28.55	15
	ST5	27.44	18
North dry rocks	ST1	26.84	n/a
	ST2	26.41	33
	ST3	30.35	33
	ST4	28.17	32
	ST5	26.21	39
Pickles reef	ST1	27.70	n/a
	ST2	26.08	34
	ST3	29.38	35
	ST4	28.85	35
	ST5	27.13	37

Table 1. Average optimum interpolation sea surface temperature (OISST) sea surface temperature (SST) and number of samples used in transcriptomic analysis (after removal of low count samples) for each sampling time point at each reef site.

seq requires lower read depth for sample quantification⁷⁹, we would like to note that our read depth is on the lower end and may affect the inference of gene processes from analysis. Despite low read depth, testing with more stringent filtering thresholds (five counts/gene in all samples, and 20 counts per gene in 80% of samples) identified the same overarching patterns and relationships in our data, with these results available in the GitHub repository.

Genet identity was the largest driver of gene expression variance

After accounting for the surrogate variable, genet identity was the largest driver of gene expression, with groupings of genet present from PC1 to PC4 (Fig. 2A–C) and no clear groupings of sampling time point (Supplementary Fig. S4) or reef site (Supplementary Fig. S5) present. Differential expression analysis, using the likelihood ratio test (LRT) method in DESeq2, identified 7,096 significant genes between the four genets (Supplementary File S3). The degreport::deggpatterns⁷² analysis, utilizing the 7,096 significant genes between the genets from the LRT, identified six different expression clusters (Supplementary File S3) with differing gene sets and expression profiles (Fig. 2D). Cluster 1 (2847 genes) showed significant GO and KEGG pathway enrichment of terms related to cell growth and protein production, with KEGG enrichment identifying multiple terms important in immune system signaling pathways (such as *RIG-I-like* (KO:04622), *C-type lectin* (KO:04625), and *NOD-like receptor* (KO:04621) *signaling pathways*), and pathogenic infection (such as *Shigellosis* (KO:05131), *Pathogenic Escherichia coli infection* (KO:05130), and *Yersinia infection* (KO:05135)) (Fig. 2E). Genet HS1 showed a strong positive association, and genet CN4 showed a strong negative association with Cluster 1 (Fig. 2D). Cluster 2 (751 genes) identified enrichment of one GO term, *Fibroblast growth factor receptor signaling* (GO:0008543), and one KEGG term, *Lysosome* (KO:04142). Genet CN4 again showed a strong negative association, and ML2 showed a strong positive association with Cluster 2 (Fig. 2D). Cluster 3 (565 genes) showed GO enrichment of ribosome and translational processes. Enrichment map analysis of the KEGG enrichment results identified one functional group: terms linked to neurodegenerative diseases (Fig. 2E and Supplementary Fig. S6A) with genet CN2 showing a strong positive association and HS1 showing a strong negative association (Fig. 2D). Cluster 4 (1421 genes) again showed GO enrichment of terms linked to ribosomes and translational processes. Enrichment map analysis of significant KEGG pathways identified two functional groups; terms linked to pathogenic infection, and terms linked to neurodegenerative diseases (Fig. 2E and Supplementary Fig. S6B). CN2 and HS1 showed negative associations with Cluster 4, while CN4 and ML2 showed positive associations (Fig. 2D). Cluster 5 (640 genes) showed no significant GO or KEGG enrichment, with genet CN2 showing a strong negative association and genet HS1 showing a strong positive association (Fig. 2D). Cluster 6 (551 genes) showed no GO enrichment, but KEGG enrichment and enrichment map analysis again identified the majority of terms to be present in a functional group linked to neurodegenerative diseases (Fig. 2E and Supplementary Fig. S6C). Genet ML2 showed a negative association and CN2 showed a positive association with Cluster 6 (Fig. 2D). Full GO enrichment and KEGG pathway enrichment results are available in Supplementary File S4 and Supplementary File S5 respectively. Venn diagram analysis identified that despite there being significant enrichment of similar neurodegenerative disease terms in Clusters 1, 3, 4, and 6, there was minimal overlap of the genes causing enrichment of these terms between the clusters, with no genes shared between all four of the clusters (Supplementary Fig. S6D).

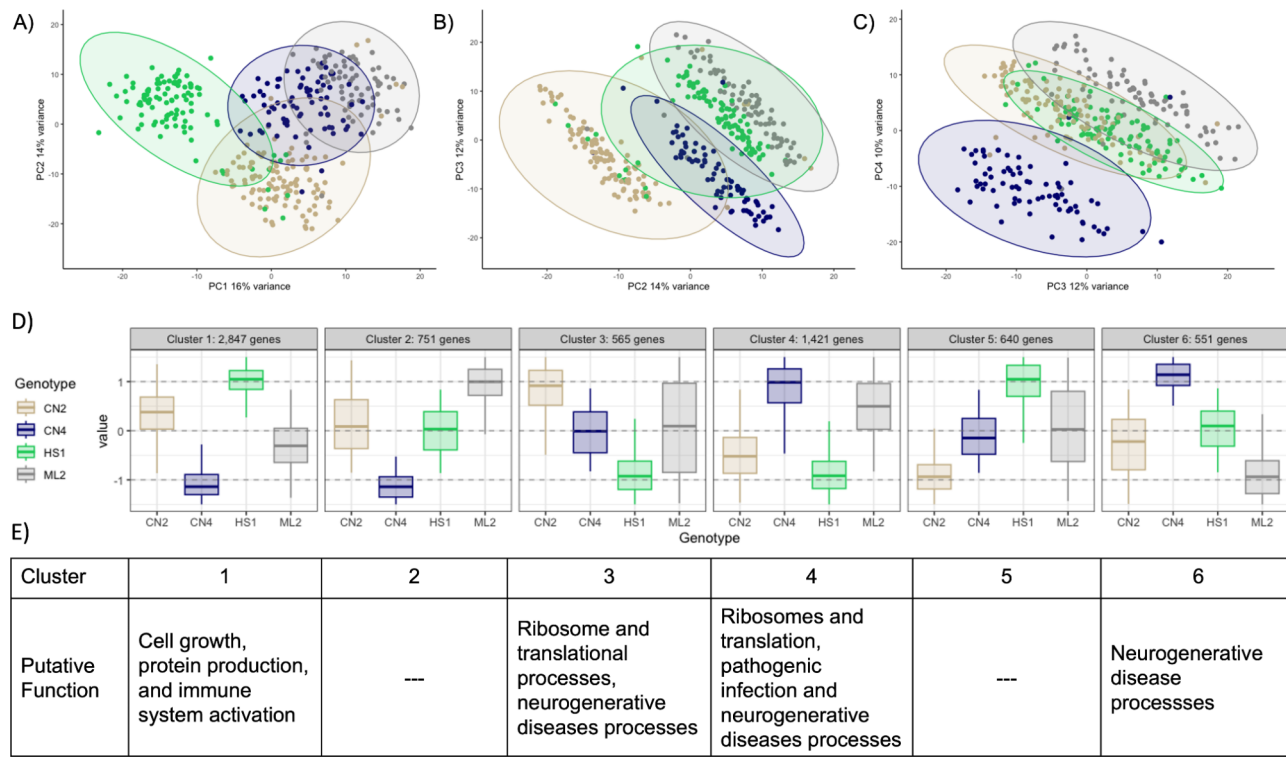
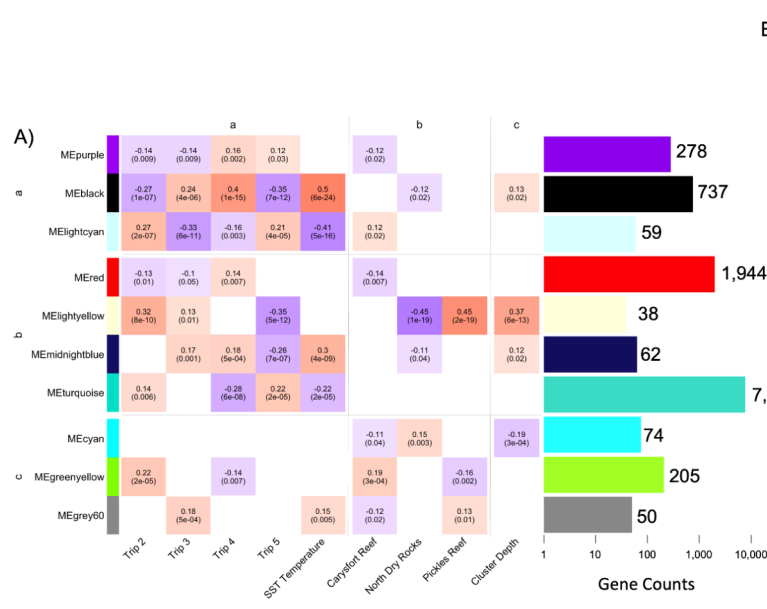


Fig. 2. Genet identity was the largest driver of gene expression variance, with expression profile clusters identifying different baseline expressions among genets. (A) Principal component (PC) 1 (16% variance) and PC2 (14% variance) of the four genets with 95% confidence intervals. (B) PC 2 (14% variance) and PC3 (12% variance) of the four genets with 95% confidence intervals. (C) PC 3 (12% variance) and PC4 (10% variance) of the four genets with 95% confidence intervals. (D) The six identified clusters from degreport::degtpattern of the significant LRT genes identified between the four genets. Each box identifies a cluster, with the x-axis showing the genet, and the y-axis the computed expression z-score for each genet. A value closer to 1 indicates higher expression, a value closer to 0 indicates neutral expression, and a value closer to -1 indicates lower expression. (E) Inferred function identified from GO and KEGG enrichment analysis for each cluster. Cells with “—” indicate no inferred function due to low or no significantly enriched GO or KEGG terms. For (A)–(D); tan = genet CN2, blue = genet CN4, green = genet HS1, and gray = genet ML2.

Co-expression analysis identified modules that significantly correlated to the winter (ST2 and ST5) and summer (ST3 and ST4) seasons once accounting for genet variance

On removal of the identified surrogate variable and genet identity, co-expression analysis identified 15 co-expression modules (Supplementary Fig. S7) ranging from 50 to 7514 genes (Supplementary File S6). Three modules showed significant correlations with all four sampling timepoints (Fig. 3A). The Purple module (278 genes, hub gene = *60S Ribosomal*) showed negative correlations with ST2 and ST3 (-0.14 and -0.14 respectively) and positive correlations with ST4 and ST5 (0.16 and 0.12 respectively) (Fig. 3A). GO and KEGG enrichment analyses identified terms to be linked to ribosomal and metabolic processes (Supplementary Files S7 and S8 respectively). From significant GO and KEGG enrichment results, the putative function of the purple module was deemed to be “*protein synthesis and homeostatic processes*”. The Black module (737 genes, hub gene = *HIG1 domain family member 1C*) showed negative correlations with ST2 and ST5 (-0.27 and -0.41 respectively), and positive correlations to ST3, ST4 (0.24 and 0.4 respectively), and SST (0.5) (Fig. 3A). GO enrichment identified only one significantly enriched term, *Endoplasmic reticulum and chaperone complex* (GO:0034663) (Supplementary File S7). KEGG enrichment identified several signaling pathways important in general cell proliferation, management, and cell growth. Specifically, this included signaling pathways (*MAPK signaling pathway* (KO:04010), *PI3K-Akt signaling pathway* (KO:04151), *GnRH signaling pathway* (KO:04912), *Ras signaling pathway* (KO:04014), and *cAMP signaling pathway* (KO:04024)) and other terms (*Focal adhesion* (KO:04510), *Proteoglycans in cancer* (KO:05205), and *Protein processing in endoplasmic reticulum* (KO:04141)) (Supplementary File S8). From significant GO and KEGG enrichment results, the putative function of the Black module was assigned as “*Organismal cellular maintenance and growth*”. The Light Cyan module (59 genes, hub gene = *Cell Surface hyaluronidase*) showed positive correlations with ST2 and ST5 (0.27 and 0.21 respectively) and negative correlations with ST3, ST4 (-0.44 and -0.16 respectively), and SST (-0.41) (Fig. 3A). There was only significant KEGG enrichment for one term: *Rheumatoid arthritis* (KO:05323) (Supplementary File S8). Due to low GO and KEGG enrichment, no putative function was assigned to the Light Cyan module.

Four modules showed significant correlations to three of the four sampling timepoints: Red, Light Yellow, Midnight Blue, and Turquoise (Fig. 3A). The Red module (1944 genes, hub gene = *Protein CREG1*) showed



Module	Hub Gene	Putative Function
Purple	60S ribosomal protein L13	Protein Synthesis and Homeostatic Processes
Black	HIG1 domain family member 1C	Organismal cellular maintenance and growth
Light Cyan	Cell surface hyaluronidase	---
Red	Protein CREG1	Mitochondrial Maintenance and Breakdown
Light Yellow	Cryptochrome-1	Metabolic Processes
Midnight Blue	Bromodomain-containing protein 2	---
Turquoise	Myosin-10	General Organism Homeostasis
Cyan	Uncharacterized protein LOC111326987	Growth Processes
Green Yellow	Golgin subfamily A member 4	Ribosome and Translational Processes
Grey 60	Putative RNA-directed DNA polymerase from transposon BS	---

Fig. 3. There were significantly correlated co-expression modules to sampling time point and reef location when accounting for genet variance. (A) Heatmap of co-expression modules and their respective correlation and significance to metadata variables of interest. Columns are split into a) sampling time point 2–5 and average OISST, b) reef locations, and c) cluster outplant depth. Heatmap rows are split into sets of co-expression modules. The heatmap fill; red = positive correlation, blue = negative correlation. Text in each cell identifies the Pearson correlation (upper value) and p-value (lower value). White cells denote a significance of > 0.05 and were removed. Bar chart to the right of the heatmap indicates the number of genes in each respective co-expression module. (B) Identified hub gene and putative function of each module as ascertained from significant GO and KEGG enrichment pathway analyses. Full GO and KEGG enrichment results used to infer function are available in Supplementary Files S7 and S8 respectively.

negative correlations with ST2 and ST3 (-0.13 and -0.1 respectively) and a positive correlation with ST4 (0.14) (Fig. 3A). GO enrichment identified three terms all linked to the mitochondrion (Supplementary File S7), while KEGG enrichment identified two main sets of processes: fatty acid metabolic processes and viral associated infections and responses (Supplementary File S8). From significant GO and KEGG enrichment results, the putative function of the Red Module was assigned as “*Mitochondrial Maintenance and Breakdown*”. The Light-Yellow module (38 genes, hub gene = *Cryptochrome-1*) showed positive correlations with ST2 and ST3 (0.32 and 0.13 respectively) and a negative correlation with ST5 (-0.35) (Fig. 3A). There was no KEGG enrichment, but GO enrichment identified terms linked to multiple parts of the mitochondrion, as well processes important in fatty acid metabolism, vitamin metabolism, and respiration (Supplementary File S7). From significant GO enrichment results, putative function of the Light-Yellow module was assigned as “*Metabolic Processes*”. The Midnight-Blue module (62 genes, hub gene = *Bromodomain containing protein 2*) showed positive correlations with ST3, ST4 and SST (0.17 , 0.18 , and 0.3 respectively) and a negative correlation with ST5 (-0.26) (Fig. 3A). There was no significant GO or KEGG enrichment for this module, thus no putative function was assigned. The Turquoise module (7,415 genes, hub gene *Myosin-10*) showed positive correlations with ST2 and ST5 (0.14 and 0.22 respectively) and negative correlations with ST4 and SST (-0.289 and -0.22 respectively) (Fig. 3A). At alpha 0.01, there were 204 significant GO terms (Supplementary File S7) and 192 significant KEGG terms (Supplementary File S8). Both GO and KEGG pathway showed enrichment of terms linked to metabolic processes, immune signaling pathways, and protein synthesis. Due to high significant enrichment of GO and KEGG terms, the turquoise module was designated as “*general organism homeostasis*”.

There were no co-expression modules that were significantly correlated to all three reef sites

Co-expression analysis identified two modules that showed correlation to at least two of the three reef sites; Light Yellow module (38 genes, hub gene = *Cryptochrome 1*) which showed a negative correlation to North Dry Rocks (-0.45) and a positive correlation to Pickles Reef (0.45), and the Cyan module (784 genes, hub gene = *uncharacterized protein LOC111326987*) which showed a negative correlation to Carysfort (-0.11) and a positive correlation to North Dry Rocks (0.15) (Fig. 3A). The Light Yellow module was assigned the putative function of “*metabolic process*” from GO and KEGG enrichment analysis. For the Cyan module, GO enrichments identified terms linked to the extracellular space as well as terms important in general organism

growth and nervous system cell development (Supplementary File S7). KEGG enrichment only identified two terms: *Maturity onset diabetes of the young* (KO:04950) and *Notch signaling pathway* (KO:04330) (Supplementary File 8). The putative function of the Cyan module was “growth processes”.

Discussion

Baseline immune gene expression and putative protein production drove differences in gene expression between the four genets

In this study, we identified that genet identity is the largest driver of gene expression in outplanted *A. palmata* (Fig. 2A-C), and this masks the signals of sampling time point and reef location. From our GO and KEGG enrichment analysis, we identified that baseline immune gene expression seems to be an important difference between genets of *A. palmata*. Baseline gene expression of an organism can be described as the normal expression levels of an organism not exposed to stimuli. Within a species, different levels of baseline expression can therefore exist for different processes. For example, differing levels of immunity between genets could drive factors such as disease susceptibility and resistance. For corals, it is well documented that there are differences in the production of immune-related molecules^{80,81} as well as differing levels of disease susceptibility^{82–84}. This also holds true within coral species, with different genets showing differing levels of susceptibility to disease^{35,36}, and heat stress^{33,34}. At present, the exact molecular mechanism(s) of differences in baseline immune activity has not been fully elucidated within a coral species. Epigenetic modification could play a role, with histone modification⁸⁵ and DNA methylation⁸⁶ being shown to influence immune gene expression in other organisms. In corals, epigenetic modifications can occur due to environmental perturbations⁸⁷ as well as specific stress such as nutrients⁸⁸. Similarly, previous work has shown that corals can front-load genes, allowing them to resist stressful conditions^{42,89}. We therefore hypothesize that different genets of *A. palmata* could be using these processes to cause differences in baseline immune gene expression. We previously showed this same difference in immune-related gene expression *A. palmata* genets in an *ex-situ* disease experiment⁶⁰. In this study, using the same four genets of *A. palmata*, we identified the same signal for baseline immune gene expression. This indicates that this signal is consistent over time and space, and is therefore important in patterns of resistance and susceptibility in *A. palmata* genets.

The clusters identified from the genet LRT analysis also identified consistent enrichment of GO terms linked to ribosome and translational processes (clusters 3 and 4). These results could indicate that among *A. palmata* genets different baseline rates of protein synthesis exist, which could affect physiological variables such as growth rates, as well as responses to biotic and abiotic perturbations. High baseline ribosome and translational processes could be linked to faster-growing genets. Specifically, we think genet CN2 may have faster growth rates in reefs as it showed higher abundances of genes involved in both ribosome and translational and growth processes (cluster 1) but additional work needs to be conducted to provide evidence for this hypothesis.

Clusters 4 and 6 both had designations for neurodegenerative diseases, with enrichment map analysis showing high connectivity for these terms (Supplementary Fig. 6A-C). Interestingly, the intersection of the genes within the highly connected neurodegenerative terms for each cluster had minimal overlap among genets (Supplementary Fig. 6D) indicating that different cellular processes are being expressed among the genets. Neurodegenerative diseases are characterized by processes such as misfolded proteins^{90,91}, oxidative stress^{92,93}, disruption of calcium homeostasis^{94,95}, and mitochondrial dysfunction^{96,97}. While these terms are specifically linked to human neurodegenerative diseases, the core processes and pathways that are involved in these diseases are present throughout the metazoan tree of life. For example, oxidative phosphorylation is a core organismal process that generates adenosine-triphosphate, the source of energy at a cellular level. Stony coral tissue loss disease research has also identified enrichment of neurodegenerative diseases term⁹⁸ which indicates that the core processes present in well-studied human diseases may show different baseline expression in different coral genets, and thus provide benefits and tradeoffs. Future work should look to fully characterize the potential pathways and processes which are encompassed in these human neural diseases in corals, and subsequently identify how these processes affect the physiological processes of corals, and if this confers any benefits or tradeoffs that can be incorporated into coral restoration projects.

The results from this study, paired with past research, underline the importance of not only characterizing the immune repertoire of coral species but also identifying how differences in baseline gene expression among coral genets may influence susceptibility and resistance to biotic and abiotic stressors. From a coral restoration perspective by characterizing the baseline immune performance, outplanting of more genets that can mount a higher immune response may improve survivorship and restoration of reefscape.

Co-expression analysis identifies higher potential growth genes in *A. palmata* in the cooler winter months and shifts to survival and defensive processes in the summer months

Once accounting for genet identity, WGCNA⁷³ analysis identified co-expression modules significantly correlated to sampling time point with three significant modules (Purple, Black Light Cyan) for the four sampling timepoints (Fig. 3A). The Black and the Light Cyan module correlations mirrored the summer versus winter months, with correlations also to sea surface temperature (Fig. 3A). The Light Cyan module, which was negatively correlated with temperature, may encompass important genes involved in growth processes in *A. palmata*. For instance, the Light Cyan module included genes involved in structural integrity of the extracellular space (collagen genes), and tissue rigidity (tricholycin and reticulobulin genes). The hub gene of this module (*cell surface hyaluronidase*) has also been shown to be important in regulation of cell adhesion, as well as the degradation of hyaluronan which regulates development and structural integrity in the extracellular matrix^{99,100}. A hyaluronan-like substance has been identified previously in the coral species *Mycetophyllia resi* with the putative function important in tissue and skeletal matrix structure¹⁰¹. This could indicate that during the cooler winter months, growth processes are

favored by outplanted *A. palmata* on the reef system, which aligns with previous findings that *A. palmata* grows quicker at cooler temperatures¹⁰².

The Black module showed the inverse compared to the Light Cyan module, with a strong positive correlation (0.5) with sea surface temperatures and sampling time points 3 and 4 (i.e., summer months) (Fig. 3A) and an inferred function of immune, survival, and metabolic processes (Fig. 3B). The survival and metabolic inferred function was identified due to the significant enrichment of the MAPK, PI3/AKT, and RAS signaling pathways. MAPK signaling is a highly conserved signaling pathway¹⁰³ with importance in gene expression, mitosis, metabolism, immune responses, and survivability¹⁰⁴. The PI3/AKT signaling pathway is similar, being highly conserved¹⁰⁵ and playing key roles in the immune system, growth, and survival¹⁰⁶. The RAS signaling pathway plays key roles in regulation and proper function of both the MAPK and PI3/AKT signaling pathways¹⁰⁷. The enrichment of these pathways during the warmer summer months suggests that outplanted *A. palmata* may shift to a more survival and maintenance mode compared to growth processes that occur in the winter. This is plausible and indicates that although *A. palmata* were not exhibiting bleaching and looked relatively healthy, even moderate increases in temperature may induce stress^{108,109}. Increased water temperatures can increase abundance and pathogen virulence^{110–112} which may explain the increased immune system expression targeted to prevent infection. While we observed differences in baseline immune gene expression between the genets, this does not limit all genets initiating immune responses to factors such as pathogens in the environment. Rather, it may influence variables such as survivability and disease resistance for specific genets, with higher baseline expression of these immune pathways conferring higher resistance to all, or specific, diseases. The Black module also contained immune signaling pathways and processes adding support to this observation. The TNF signaling pathway is an important immune cytokine that can activate additional innate immune responses¹¹³, is important in cell proliferation and cell death¹¹⁴, and consistently shows increased expression in coral disease^{98,115,116} and heat^{117,118} transcriptomic studies.

Reef location did not have a strong effect on gene expression for outplanted genets of *Acropora palmata*

Principal component analysis and co-expression analysis did not identify a strong effect of the outplant reef site on gene expression between the four genets of *A. palmata*. There were two co-expression modules that did show significant correlations to at least two of the three reef sites as well as cluster outplant depth (Fig. 3A). There was only significant GO enrichment for the Light Yellow module, with terms involved in mitochondrial processes and fatty acid metabolism (Supplementary File 7). Coral species are mixotrophic utilizing both autotrophic processes, where energy is derived from photosynthates produced by the obligate symbiont *Symbiodinaceae*, and heterotrophic processes, involving passive and active means of acquiring energy. Light availability is the key variable that dictates the level of these factors. Light availability however can be affected by not only depth, but turbidity of the reef site, with more shallow reef sites that exhibit higher levels of turbidity having reduced light availability for autotrophic energy acquisition. Despite this, coral species at deeper depths (i.e. species that inhabit shallow to upper mesophotic reef depths ~ 60m) switch to a more heterotrophic lifestyle mode of energy acquisition due to the lower levels of light available causing decreased output from the photosynthetic *Symbiodinaceae*¹¹⁹. With the significant correlation to depth, it is plausible that outplanted *A. palmata* at Pickles Reef could rely more heavily on heterotrophic energy acquisition processes. However, this hypothesis requires substantial additional testing. As we only measured outplant depth we cannot disentangle whether this is truly due to outplant depth and light availability, or whether other variables such as turbidity (which can influence light availability), or water flow regime, could be driving this result. Enrichment of fatty acid metabolic processes in the Light Yellow module do however provide additional support for our hypothesis. Corals living at deeper depths in a more heterotrophic lifestyle have been shown to have higher energy reserves than corals at shallow depths in a more autotrophic lifestyle^{120,121}. The outplanted *A. palmata* at Pickles may therefore be utilizing fatty acid stores that they have acquired through higher rates of heterotrophic feeding. While we pose this hypothesis, we do acknowledge that it is not possible to directly compare mesophotic to shallow coral reefs due to a wide range of differences in the abiotic and biotic variables present. Specifically abiotic variables (such as light availability and temperature¹²²) and biotic variables (such as symbiont density¹²³ and growth rates^{124,125}) vary greatly between these reef habitats. To fully test this hypothesis, incorporation of reef sites spreading the full range between shallow and mesophotic reefs would be needed, with a full range of abiotic variables (temperature, outplant depth, turbidity, water flow regime) and biotic (symbiont density, growth rates, microbiome composition) needed to disentangle whether light availability is causing shifts in energy acquisition. Additionally, utilization of methodologies such as whole tissue stable isotope analysis of carbon and nitrogen, as well as tissue lipid content analysis, in conjunction with measured abiotic and biotic variables, would allow a more definitive conclusion of how shifts in levels of heterotrophic and autotrophic energy acquisition may change in outplanted *A. palmata*.

Conclusions and future directions for genomic analysis of outplanted corals

We identified that genet identity is an important factor in outplanted *A. palmata*, and a leading driver of the differences seen between the four genets is baseline immune gene expression. Since we identified an intra-population variation in response to phenotypically healthy corals, more *A. palmata* genets would help identify whether this pattern holds at a population level. While it was only possible to include four genets in this current analysis, incorporation of samples of the additional seven genets taken during the fieldwork portion of this project would be a good starting point. Using a larger sample genet sample size would allow to identify how baseline profiles influence outplant performance. Additional *ex-situ* experiments of multiple genets of *A. palmata* to different biotic and abiotic stressors would also help identify the “winner” and “loser” genets. These results could be incorporated into restoration practices potentially increasing outplant survivability by matching fitter genets to preferred reef systems.

Future work looking at the effects of outplant sites on coral gene expression should include a wider range of reef habitats. Despite the reef habitats used in this study exhibiting different topologies and rugosity, they are all still offshore reef sites within close proximity. Inshore and offshore reef systems have been shown to have different abiotic conditions influencing the performance of resident coral populations. By monitoring outplanted coral at different reef systems with different abiotic conditions, it would allow characterization of gene pathways that are affected due to these environmental conditions.

Data availability

All analysis scripts and pipelines can be found at https://github.com/benyoung93/acropora_palmata_field_transcriptomics, with all RNA-seq raw reads available on the NCBI under accession under PRJNA1081901.

Received: 12 April 2024; Accepted: 19 November 2024

Published online: 27 November 2024

References

1. Hoegh-Guldberg, O. Coral reef ecosystems and anthropogenic climate change. *Reg. Environ. Change.* **11**, 215–227 (2011).
2. Hoegh-Guldberg, O., Poloczanska, E. S., Skirving, W. & Dove, S. Coral Reef Ecosystems under Climate Change and Ocean Acidification. *Front. Mar. Sci.* **4**, (2017).
3. Hughes, T. P. et al. Global warming and recurrent mass bleaching of corals. *Nature* **543**, 373–377 (2017).
4. Tracy, A. M., Weil, E. & Harvell, C. D. Warming and pollutants interact to modulate octocoral immunity and shape disease outcomes. *Ecol. Appl.* **30**, e02024 (2020).
5. Redding, J. E. et al. Link between sewage-derived nitrogen pollution and coral disease severity in Guam. *Mar. Pollut Bull.* **73**, 57–63 (2013).
6. Zaneveld, J. R. et al. Overfishing and nutrient pollution interact with temperature to disrupt coral reefs down to microbial scales. *Nat. Commun.* **7**, 11833 (2016).
7. Sutherland, K. P. et al. Human sewage identified as likely source of white pox disease of the threatened Caribbean elkhorn coral, *Acropora palmata*: likely human sewage source of white pox disease of elkhorn coral. *Environ. Microbiol.* **12**, 1122–1131 (2010).
8. Skirving, W. J. et al. The relentless march of mass coral bleaching: a global perspective of changing heat stress. *Coral Reefs.* **38**, 547–557 (2019).
9. Hughes, T. P. et al. Spatial and temporal patterns of mass bleaching of corals in the Anthropocene. *Science* **359**, 80–83 (2018).
10. Anthony, K. R. N. Coral Reefs under Climate Change and Ocean Acidification: challenges and opportunities for Management and Policy. *Annu. Rev. Environ. Resour.* **41**, 59–81 (2016).
11. Chan, N. C. S. & Connolly, S. R. Sensitivity of coral calcification to ocean acidification: a meta-analysis. *Glob Change Biol.* **19**, 282–290 (2013).
12. Dove, S. G., Brown, K. T., Van Den Heuvel, A., Chai, A. & Hoegh-Guldberg, O. Ocean warming and acidification uncouple calcification from calcifier biomass which accelerates coral reef decline. *Commun. Earth Environ.* **1**, 1–9 (2020).
13. Burkepile, D. E. et al. Nitrogen Identity drives Differential impacts of nutrients on Coral Bleaching and Mortality. *Ecosystems* **23**, 798–811 (2020).
14. Vega Thurber, R. L. et al. Chronic nutrient enrichment increases prevalence and severity of coral disease and bleaching. *Glob Change Biol.* **20**, 544–554 (2014).
15. Bruno, J. F., Sweatman, H., Precht, W. F., Selig, E. R. & Schutte, V. G. W. assessing evidence of phase shifts from coral to macroalgal dominance on coral reefs. *Ecology* **90**, 1478–1484 (2009).
16. Graham, N. A. et al. Managing resilience to reverse phase shifts in coral reefs. *Front. Ecol. Environ.* **11**, 541–548 (2013).
17. Dudgeon, S. R., Aronson, R. B., Bruno, J. F. & Precht, W. F. Phase shifts and stable states on coral reefs. *Mar. Ecol. Prog. Ser.* **413**, 201–216 (2010).
18. Boström-Einarsson, L. et al. Coral restoration – A systematic review of current methods, successes, failures and future directions. *PLOS ONE* **15**, e0226631 (2020).
19. Omori, M. Coral restoration research and technical developments: what we have learned so far. *Mar. Biol. Res.* **15**, 377–409 (2019).
20. Hein, M. Y. et al. Coral restoration effectiveness: multiregional snapshots of the long-term responses of Coral assemblages to Restoration. *Diversity* **12**, 153 (2020).
21. Fox, H. E. et al. Rebuilding coral reefs: success (and failure) 16 years after low-cost, low-tech restoration. *Restor. Ecol.* **27**, 862–869 (2019).
22. Page, C. A., Muller, E. M. & Vaughan, D. E. Microfragmenting for the successful restoration of slow growing massive corals. *Ecol. Eng.* **123**, 86–94 (2018).
23. Knapp, I. S. S. et al. Coral micro-fragmentation assays for optimizing active reef restoration efforts. *PeerJ* **10**, e13653 (2022).
24. Forsman, Z. H., Page, C. A., Toonen, R. J. & Vaughan, D. Growing coral larger and faster: micro-colony-fusion as a strategy for accelerating coral cover. *PeerJ* **3**, e1313 (2015).
25. Martínez-Castillo, V. & Rodríguez-Troncoso, A. P. Cupul-Magaña, A. L. Evidence of sexual Reproduction in Out-Planted Coral colonies. *Oceans* **4**, 350–359 (2023).
26. Williams, D. E., Bright, A. J., Williamson, O. M., Moura, A. & Ladd, M. C. Synchronous spawning of nursery-raised elkhorn coral (*Acropora palmata*) outplanted to reefs in the Florida Keys (United States). *Front. Mar. Sci.* **10**, (2023).
27. Walther, B. D., Kingsford, M. J. & McCulloch, M. T. Environmental Records from great barrier reef corals: Inshore versus Offshore drivers. *PLOS ONE* **8**, e77091 (2013).
28. Sillapathivong, A. & True, J. Different coral compositions reflect contrasting environmental patterns of inshore and offshore reef habitats in Thailand. *Songklanakarin J. Sci. Technol. SJST.* **40**, 179–185 (2018).
29. Manzello, D. P., Enochs, I. C., Kolodziej, G. & Carlton, R. Recent decade of growth and calcification of *Orbicella faveolata* in the Florida Keys: an inshore-offshore comparison. *Mar. Ecol. Prog. Ser.* **521**, 81–89 (2015).
30. Lartaud, F. et al. Springer International Publishing, Cham., Growth Patterns in Long-Lived Coral Species. in Marine Animal Forests: The Ecology of Benthic Biodiversity Hotspots (eds. Rossi, S., Bramanti, L., Gori, A. & Orejas Saco del Valle, C.) 1–32 doi: (2015). https://doi.org/10.1007/978-3-319-17001-5_15-1
31. Madin, J. S. et al. Selecting coral species for reef restoration. *J. Appl. Ecol.* **60**, 1537–1544 (2023).
32. Henley, E. M. et al. Growth and survival among hawaiian corals outplanted from tanks to an ocean nursery are driven by individual genotype and species differences rather than preconditioning to thermal stress. *PeerJ* **10**, e13112 (2022).
33. Drury, C. & Lirman, D. Genotype by environment interactions in coral bleaching. *Proc. R Soc. B Biol. Sci.* **288**, 20210177 (2021).
34. Dziedzic, K. E., Elder, H., Tavalire, H. & Meyer, E. Heritable variation in bleaching responses and its functional genomic basis in reef-building corals (*Orbicella faveolata*). *Mol. Ecol.* **28**, 2238–2253 (2019).

35. Miller, M. W. et al. Genotypic variation in disease susceptibility among cultured stocks of elkhorn and staghorn corals. *PeerJ* **7**, e6751 (2019).
36. Müller, E. M., Bartels, E. & Baums, I. B. Bleaching causes loss of disease resistance within the threatened coral species *Acropora cervicornis*. *eLife* **7**, e35066 (2018).
37. Drury, C., Manzello, D. & Lirman, D. Genotype and local environment dynamically influence growth, disturbance response and survivorship in the threatened coral, *Acropora cervicornis*. *PLOS ONE* **12**, e0174000 (2017).
38. Lirman, D. et al. Growth dynamics of the threatened caribbean Staghorn Coral *Acropora cervicornis*: influence of Host Genotype, Symbiont identity, colony size, and Environmental setting. *PLOS ONE* **9**, e107253 (2014).
39. Ladd, M. C., Shantz, A. A., Bartels, E. & Burkepile, D. E. Thermal stress reveals a genotype-specific tradeoff between growth and tissue loss in restored *Acropora cervicornis*. *Mar. Ecol. Prog. Ser.* **572**, 129–139 (2017).
40. Gibney, E. R. & Nolan, C. M. Epigenetics and gene expression. *Heredity* **105**, 4–13 (2010).
41. Zhang, N. Role of methionine on epigenetic modification of DNA methylation and gene expression in animals. *Anim. Nutr.* **4**, 11–16 (2018).
42. Vidal-Dupiol, J. et al. Frontloading of stress response genes enhances robustness to environmental change in chimeric corals. *BMC Biol.* **20**, 167 (2022).
43. Collins, M., Clark, M. S., Spicer, J. I. & Truebano, M. Transcriptional frontloading contributes to cross-tolerance between stressors. *Evol. Appl.* **14**, 577–587 (2021).
44. Balogun, E. J. & Ness, R. W. The effects of De Novo Mutation on Gene expression and the consequences for Fitness in *Chlamydomonas reinhardtii*. *Mol. Biol. Evol.* **41**, msae035 (2024).
45. Singh, K. P., Miaskowski, C., Dhruva, A. A., Flowers, E. & Kober, K. M. Mechanisms and measurement of changes in Gene expression. *Biol. Res. Nurs.* **20**, 369–382 (2018).
46. Young, C., Schopmeyer, S. & Lirman, D. A. Review of reef restoration and Coral Propagation using the threatened Genus *Acropora* in the Caribbean and Western Atlantic. *Bull. Mar. Sci.* **88**, 1075–1098 (2012).
47. Forrester, G. E., Maynard, A., Schofield, S. & Taylor, K. Evaluating causes of transplant stress in fragments of *Acropora Palmata* used for coral reef restoration. *Bull. Mar. Sci.* **88**, 1099–1113 (2012).
48. Kuffner, I. B., Stathakopoulos, A., Toth, L. T. & Bartlett, L. A. Reestablishing a stepping-stone population of the threatened elkhorn coral *Acropora palmata* to aid regional recovery. *Endanger. Species Res.* **43**, 461–473 (2020).
49. Aronson, R. B. & Precht, W. F. White-band disease and the changing face of Caribbean coral reefs, in *The Ecology and Etiology of Newly Emerging Marine Diseases* (ed Porter, J. W.) 25–38 (Springer Netherlands, Dordrecht, doi:https://doi.org/10.1007/978-94-017-3284-0_2). (2001).
50. Randall, C. J. & van Woesik, R. Contemporary white-band disease in Caribbean corals driven by climate change. *Nat. Clim. Change* **5**, 375–379 (2015).
51. Williams, D. E., Miller, M. W., Bright, A. J., Pausch, R. E. & Valdivia, A. Thermal stress exposure, bleaching response, and mortality in the threatened coral *Acropora palmata*. *Mar. Pollut. Bull.* **124**, 189–197 (2017).
52. Gardner, T. A., Côté, I. M., Gill, J. A., Grant, A. & Watkinson, A. R. Long-term region-wide declines in Caribbean corals. *Science* **301**, 958–960 (2003).
53. Cramer, K. L. et al. Widespread loss of Caribbean acroporid corals was underway before coral bleaching and disease outbreaks. *Sci. Adv.* **6**, eaax9395 (2020).
54. Lirman, D. Fragmentation in the branching coral *Acropora palmata* (Lamarck): growth, survivorship, and reproduction of colonies and fragments. *J. Exp. Mar. Biol. Ecol.* **251**, 41–57 (2000).
55. Reynolds, R. W. et al. Daily High-Resolution-blended analyses for Sea Surface temperature. *J. Clim.* **20**, 5473–5496 (2007).
56. Banzon, V., Smith, T. M., Chin, T. M., Liu, C. & Hankins, W. A long-term record of blended satellite and in situ sea-surface temperature for climate monitoring, modeling and environmental studies. *Earth Syst. Sci. Data* **8**, 165–176 (2016).
57. Huang, B. et al. Improvements of the Daily Optimum Interpolation Sea Surface temperature (DOISST) version 2.1. *J. Clim.* **34**, 2923–2939 (2021).
58. Wickham, H. et al. Welcome to the Tidyverse. *J. Open. Source Softw.* **4**, 1686 (2019).
59. Wickham, H. *ggplot2: Elegant Graphics for Data Analysis*. (2016).
60. Young, B. D. et al. Different disease inoculations cause common responses of the host immune system and prokaryotic component of the microbiome in *Acropora palmata*. *PLOS ONE* **18**, e0286293 (2023).
61. Young, B. D. & Automated DNA/RNA Extractions from a Stony Coral (*Acropora Palmata*) Using ZymoBIOMICS DNA/RNA Magbead Kit and the Kingfisher Flex V2. <https://www.protocols.io/view/automated-dna-rna-extractions-from-a-stony-coral-a-cqnsve> doi: (2022). <https://doi.org/10.17504/protocols.io.bp2l61wykvqe/v2>
62. Bushnell, B. & BBTools (2014).
63. Andrews, S. & FastQC: A Quality Control Tool for High Throughput Sequence Data. (2010).
64. Patro, R., Duggal, G., Love, M. I., Irizarry, R. A. & Kingsford, C. Salmon provides fast and bias-aware quantification of transcript expression. *Nat. Methods* **14**, 417–419 (2017).
65. Kitchen, S. A. et al. Genomic Variants Among Threatened *Acropora* Corals. *9*, 31919109 Bytes (2019).
66. Baums, I. B. Baums Laboratory | Penn State University Marine Biology | Research in Coral Ecology and Evolution. (2018). <http://baumslab.org/>.
67. Soneson, C., Love, M. I. & Robinson, M. D. Differential analyses for RNA-seq: transcript-level estimates improve gene-level inferences [version 2; peer review: 2 approved]. *F1000 Res.* **4**, 23 (2016).
68. Murtagh, F. & Legendre, P. Ward's hierarchical agglomerative clustering method: which Algorithms Implement Ward's Criterion? *J. Classif.* **31**, 274–295 (2014).
69. Love, M. I., Huber, W. & Anders, S. Moderated estimation of Fold change and dispersion for RNA-seq data with DESeq2. *Genome Biol.* **15**, 550 (2014).
70. Blighe, K., Lun, A. & PCAtools PCAtools: Everything Principal Components Analysis. (2022).
71. Ritchie, M. E. et al. Limma powers differential expression analyses for RNA-sequencing and microarray studies. *Nucleic Acids Res.* **43**, e47–e47 (2015).
72. DEGreport. Bioconductor <http://bioconductor.org/packages/DEGreport/>
73. Langfelder, P. & Horvath, S. WGCNA: an R package for weighted correlation network analysis. *BMC Bioinform.* **9**, 559 (2008).
74. Gu, Z., Eils, R. & Schlesner, M. Complex heatmaps reveal patterns and correlations in multidimensional genomic data. *Bioinformatics* **32**, 2847–2849 (2016).
75. Shannon, P. et al. Cytoscape: a Software Environment for Integrated Models of Biomolecular Interaction Networks. *Genome Res.* **13**, 2498–2504 (2003).
76. Maere, S., Heymans, K. & Kuiper, M. BiNGO: a Cytoscape plugin to assess overrepresentation of Gene Ontology categories in Biological Networks. *Bioinformatics* **21**, 3448–3449 (2005).
77. Yu, G., Wang, L. G., Han, Y. & He, Q. Y. clusterProfiler: An R package for comparing biological themes among gene clusters. *OMICS J. Integr. Biol.* **16**, 284–287 (2012).
78. Yu, G. & enrichplot Visualization of Functional Enrichment Result. (2021).
79. Ma, F. et al. A comparison between whole transcript and 3' RNA sequencing methods using Kapa and Lexogen library preparation methods. *BMC Genom.* **20**, 9 (2019).

80. Fuess, L. E., Mann, W. T., Jinks, L. R., Brinkhuis, V. & Mydlarz, L. D. Transcriptional analyses provide new insight into the late-stage immune response of a diseased Caribbean coral. *R Soc. Open. Sci.* **5**, 172062 (2018).
81. Palmer, C. V., Mydlarz, L. D. & Willis, B. L. Evidence of an inflammatory-like response in non-normally pigmented tissues of two scleractinian corals. *Proc. R. Soc. B Biol. Sci.* **275**, 2687–2693 (2008).
82. Williams, L., Smith, T. B., Burge, C. A. & Brandt, M. E. Species-specific susceptibility to white plague disease in three common caribbean corals. *Coral Reefs.* **39**, 27–31 (2020).
83. Meiling, S. S. et al. Variable species responses to experimental Stony Coral tissue loss disease (SCTLD) exposure. *Front. Mar. Sci.* **8**, (2021).
84. MacKnight, N. J. et al. Microbial dysbiosis reflects disease resistance in diverse coral species. *Commun. Biol.* **4**, 679 (2021).
85. Li, X. et al. Histones: the critical players in innate immunity. *Front. Immunol.* **13**, 1030610 (2022).
86. Bannister, S., Messina, N. L., Novakovic, B. & Curtis, N. The emerging role of epigenetics in the immune response to vaccination and infection: a systematic review. *Epigenetics* **15**, 555–593 (2020).
87. Rodríguez-Casariego, J. A. et al. Genome-wide DNA methylation analysis reveals a conserved epigenetic response to Seasonal Environmental Variation in the Staghorn Coral *Acropora cervicornis*. *Front. Mar. Sci.* **7**, (2020).
88. Rodriguez-Casariego, J. A. et al. Coral epigenetic responses to nutrient stress: histone H2A.X phosphorylation dynamics and DNA methylation in the staghorn coral *Acropora cervicornis*. *Ecol. Evol.* **8**, 12193–12207 (2018).
89. Barshis, D. J. et al. Genomic basis for coral resilience to climate change. *Proc. Natl. Acad. Sci.* **110**, 1387–1392 (2013).
90. Li, H., Yu, Z. & Zhang, W. Misfolded protein aggregation and altered cellular pathways in neurodegenerative diseases. *STEMedicine* **1**, e63–e63 (2020).
91. Rolli, S. & Sontag, E. M. Spatial sequestration of misfolded proteins in neurodegenerative diseases. *Biochem. Soc. Trans.* **50**, 759–771 (2022).
92. Merelli, A., Repetto, M., Lazarowski, A., Auzmendi, J. & Hypoxia. Oxidative stress, and inflammation: three faces of neurodegenerative diseases. *J. Alzheimers Dis.* **82**, S109–S126 (2021).
93. Teleanu, D. M. et al. An overview of oxidative stress, Neuroinflammation, and neurodegenerative diseases. *Int. J. Mol. Sci.* **23**, 5938 (2022).
94. Ge, M. et al. Role of Calcium Homeostasis in Alzheimer's Disease. *Neuropsychiatr Dis. Treat.* **18**, 487–498 (2022).
95. Cascella, R. & Cecchi, C. Calcium dyshomeostasis in Alzheimer's Disease Pathogenesis. *Int. J. Mol. Sci.* **22**, 4914 (2021).
96. Monzio Compagnoni, G. et al. The role of Mitochondria in neurodegenerative diseases: the lesson from Alzheimer's Disease and Parkinson's Disease. *Mol. Neurobiol.* **57**, 2959–2980 (2020).
97. Johnson, J. et al. Mitochondrial dysfunction in the development and progression of neurodegenerative diseases. *Arch. Biochem. Biophys.* **702**, 108698 (2021).
98. Traylor-Knowles, N. et al. Gene expression response to Stony Coral tissue loss Disease Transmission in *M. cavernosa* and *O. faveolata* from Florida. *Front. Mar. Sci.* **8**, 681563 (2021).
99. Tobisawa, Y. et al. The cell surface hyaluronidase TMEM2 is essential for systemic hyaluronan catabolism and turnover. *J. Biol. Chem.* **297**, 101281 (2021).
100. Toole, B. P. Hyaluronan: from extracellular glue to pericellular cue. *Nat. Rev. Cancer.* **4**, 528–539 (2004).
101. Goldberg, W. M. Acid polysaccharides in the skeletal matrix and calicoblastic epithelium of the stony coral *Mycetophyllum reesi*. *Tissue Cell.* **33**, 376–387 (2001).
102. Merck, D. E., Petrik, C. G., Manfroy, A. A. & Muller, E. M. Optimizing seawater temperature conditions to increase the productivity of ex situ coral nurseries. *PeerJ* **10**, e13017 (2022).
103. Widmann, C., Gibson, S., Jarpe, M. B. & Johnson, G. L. Mitogen-activated protein kinase: conservation of a three-kinase Module from yeast to human. *Physiol. Rev.* **79**, 143–180 (1999).
104. Cargnello, M. & Roux, P. P. Activation and function of the MAPKs and their substrates, the MAPK-Activated protein kinases. *Microbiol. Mol. Biol. Rev. MMBR.* **75**, 50–83 (2011).
105. Philippon, H., Brochier-Armanet, C. & Perrière, G. Evolutionary history of phosphatidylinositol-3-kinases: ancestral origin in eukaryotes and complex duplication patterns. *BMC Evol. Biol.* **15**, 226 (2015).
106. Hemmings, B. A. & Restuccia, D. F. PI3K-PKB/Akt Pathway. *Cold Spring Harb Perspect. Biol.* **4**, a011189 (2012).
107. Zenonos, K. & Kyriyanou, K. RAS signaling pathways, mutations and their role in colorectal cancer. *World J. Gastrointest. Oncol.* **5**, 97–101 (2013).
108. Manzello, D. P. Rapid Recent Warming of Coral Reefs in the Florida Keys. *Sci. Rep.* **5**, 16762 (2015).
109. Kuffner, I. B., Lidz, B. H., Hudson, J. H. & Anderson, J. S. A century of Ocean Warming on Florida Keys Coral reefs: historic in situ observations. *Estuaries Coasts.* **38**, 1085–1096 (2015).
110. Garren, M., Son, K., Tout, J., Seymour, J. R. & Stocker, R. Temperature-induced behavioral switches in a bacterial coral pathogen. *ISME J.* **10**, 1363–1372 (2016).
111. Tout, J. et al. Increased seawater temperature increases the abundance and alters the structure of natural *Vibrio* populations associated with the coral *Pocillopora damicornis*. *Front. Microbiol.* **6**, (2015).
112. Howells, E. J., Vaughan, G. O., Work, T. M., Burt, J. A. & Abrego, D. Annual outbreaks of coral disease coincide with extreme seasonal warming. *Coral Reefs.* **39**, 771–781 (2020).
113. Holbrook, J., Lara-Reyna, S., Jarosz-Griffiths, H. & McDermott, M. F. Tumour necrosis factor signalling in health and disease. *F1000Research* **8**, F1000 Faculty Rev-111 (2019).
114. Warzocha, K. & Salles, G. The Tumor necrosis factor signaling complex: choosing a path toward cell death or cell proliferation. *Leuk. Lymphoma.* **29**, 81–92 (1998).
115. Young, B. D. et al. Innate immune gene expression in *Acropora palmata* is consistent despite variance in yearly disease events. *PLOS ONE.* **15**, e0228514 (2020).
116. MacKnight, N. J. et al. Disease resistance in coral is mediated by distinct adaptive and plastic gene expression profiles. *Sci. Adv.* **8**, eab06153 (2022).
117. Voolstra, C. R. et al. Contrasting heat stress response patterns of coral holobionts across the Red Sea suggest distinct mechanisms of thermal tolerance. *Mol. Ecol.* **30**, 4466–4480 (2021).
118. Hou, J. et al. RNA-Seq reveals extensive transcriptional response to heat stress in the Stony Coral *Galaxea fascicularis*. *Front. Genet.* **9**, (2018).
119. Tremblay, P., Maguer, J. F., Grover, R. & Ferrier-Pagès, C. Trophic dynamics of scleractinian corals: stable isotope evidence. *J. Exp. Biol.* **218**, 1223–1234 (2015).
120. Carmignani, A. et al. Levels of autotrophy and heterotrophy in mesophotic corals near the end photic zone. *Front. Mar. Sci.* **10**, (2023).
121. Alamaru, A., Loya, Y., Brokovich, E., Yam, R. & Shemesh, A. Carbon and nitrogen utilization in two species of Red Sea corals along a depth gradient: insights from stable isotope analysis of total organic material and lipids. *Geochim. Cosmochim. Acta.* **73**, 5333–5342 (2009).
122. Lesser, M. P., Slattery, M. & Leichter, J. J. Ecology of mesophotic coral reefs. *J. Exp. Mar. Biol. Ecol.* **375**, 1–8 (2009).
123. Kramer, N. et al. Efficient light-harvesting of mesophotic corals is facilitated by coral optical traits. *Funct. Ecol.* **36**, 406–418 (2022).
124. Pinheiro, H. T., Eyal, G. & Shepherd, B. Rocha, L. A. Ecological insights from environmental disturbances in mesophotic coral ecosystems. *Ecosphere* **10**, e02666 (2019).

125. Kahng, S. E. et al. in *Light, Temperature, Photosynthesis, Heterotrophy, and the Lower Depth Limits of Mesophotic Coral Ecosystems*. 801–828 (eds Mesophotic Coral Ecosystems, Y., Puglise, K. A. & Bridge, T. C. L.) (Springer International Publishing, 2019). https://doi.org/10.1007/978-3-319-92735-0_42.

Acknowledgements

We would like to thank Caroline Dennison, Dr. Allyson DeMerlis, Samara Neufeld, and Dr. Ana Palacio-Castro for helping collect samples of *Acropora palmata* in the field. We would also like to thank all the staff at the Huntsman Institute for Human Genomics (University of Miami, Miami), for sample quality control and sequencing. We also thank Dr. Sheila Kitchen and Dr. Iliana Baums for continued use of the *Acropora palmata* genome. Finally, we thank the NOAA 'Omics OAR NO_0019 for providing funding support for molecular lab work, sequencing, and support for Stephanie Rosales and Benjamin Young. This research was carried out, in part, under the auspices of the Cooperative Institute for Marine and Atmospheric Studies, a cooperative institute of the University of Miami, and the National Oceanic and Atmospheric Administration (NOAA), cooperative agreement NA 20OAR4320472.

Author contributions

Initial study conception was SMR, with RNA-seq sample choice by SMR, BDY, and NTK. DW, AB, AP, SMR, BDY all performed fieldwork and field coral processing. BDY performed all lab work and bioinformatic analyses. BDY wrote the first draft of the manuscript, with all authors then providing feedback and edits before submission for peer review and publication.

Declarations

Competing interests

The authors declare no competing interests.

Additional information

Supplementary Information The online version contains supplementary material available at <https://doi.org/10.1038/s41598-024-80479-y>.

Correspondence and requests for materials should be addressed to B.D.Y.

Reprints and permissions information is available at www.nature.com/reprints.

Publisher's note Springer Nature remains neutral with regard to jurisdictional claims in published maps and institutional affiliations.

Open Access This article is licensed under a Creative Commons Attribution-NonCommercial-NoDerivatives 4.0 International License, which permits any non-commercial use, sharing, distribution and reproduction in any medium or format, as long as you give appropriate credit to the original author(s) and the source, provide a link to the Creative Commons licence, and indicate if you modified the licensed material. You do not have permission under this licence to share adapted material derived from this article or parts of it. The images or other third party material in this article are included in the article's Creative Commons licence, unless indicated otherwise in a credit line to the material. If material is not included in the article's Creative Commons licence and your intended use is not permitted by statutory regulation or exceeds the permitted use, you will need to obtain permission directly from the copyright holder. To view a copy of this licence, visit <http://creativecommons.org/licenses/by-nc-nd/4.0/>.

© The Author(s) 2024